Supporting Information:

Influence of Binding Site Affinity Patterns on Binding of Multivalent Polymers

Emiko Zumbro and Alfredo Alexander-Katz*

Department of Materials Science and Engineering, Massachusetts Institute of Technology, 77 Massachusetts Ave, Cambridge, MA

E-mail: aalexand@mit.edu

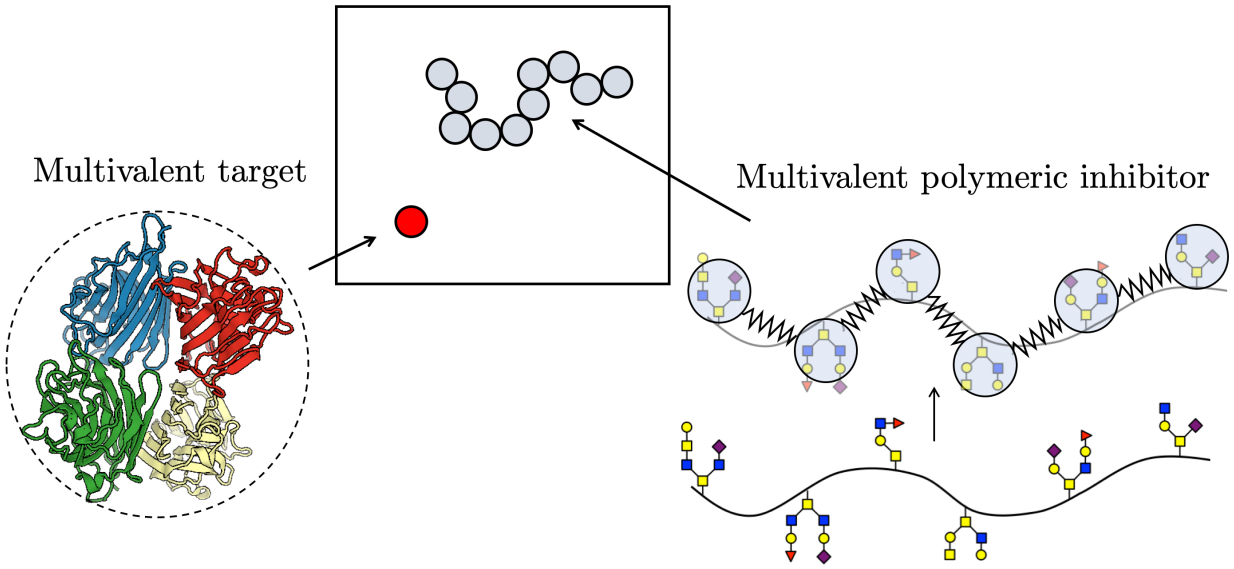

Figure S1: Schematic of simulation. The globular protein target is approximated as a sphere with one or more binding sites. The polymeric inhibitor is represented by a bead spring model where each bead has a single binding site and is connected to its neighbors through harmonic springs. Rendering from the Protein Data Bank.[1,2] This figure is reprinted from Zumbro *et al.* with permission from Elsevier.[3]

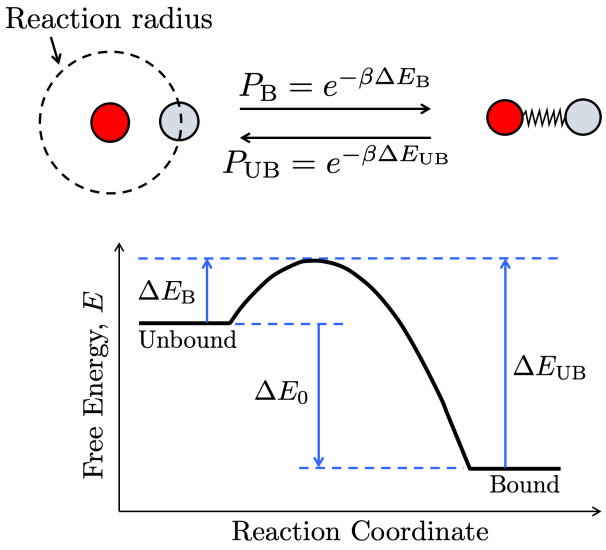

Figure S2: Depiction of reactive binding scheme for simulation. If the target (red) is within the reaction radius of a polymer bead (grey), there is a probability of binding P_{B} based on the defined energy barrier. Once bound, there is some probability of unbinding P_{UB} based on the specified energy barrier. This figure is reprinted from Zumbro *et al.* with permission from Elsevier.[3]

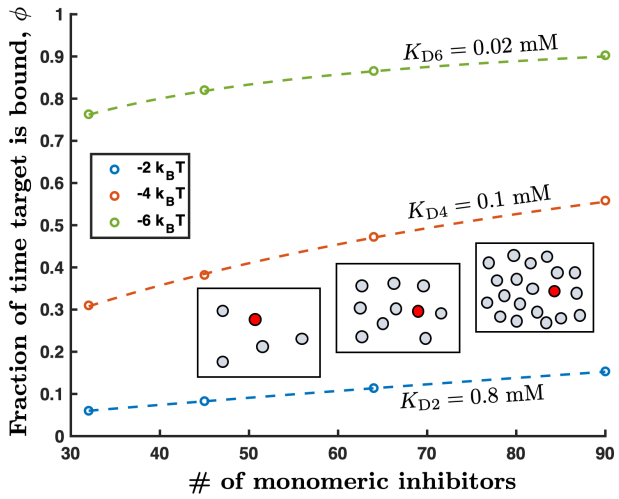

Figure S3: Simulated fraction of time bound for a monovalent target binding to monomeric inhibitor beads shown as points (o), with fitted Langmuir adsorption curve shown in dashed line (- - -). The K_{D}s shown are estimated using the fitted adsorption curve for $\Delta E_0 = -2k_{\mathrm{B}}T$ (blue), $-4k_{\mathrm{B}}T$ (orange), and $-6k_{\mathrm{B}}T$ (green).

1 Monovalent binding affinity

To confirm that we used biologically relevant binding affinities for individual binding site interactions, we placed increasing concentrations of monovalent inhibitor beads in a box with a single monovalent target. At each concentration of inhibitor beads, we measured the fraction of time the target spent bound ϕ. The plot of the fraction of time the target spent bound versus the inhibitor bead concentration is shown in Fig. S3. To estimate the K_{D} of binding, we fit our simulation data with the Langmuir adsorption curve $\phi = \frac{[I]}{[I]+K_{\mathrm{D}}}$ where $[I]$ is the concentration of inhibitor beads and K_{D} is the dissociation constant of the binding reaction. We converted our unitless K_{D} to a concentration in Molar by estimating our target diameter to be approximately 5 nm.[4]

This method resulted in a $K_{\mathrm{D}} = 8{\times}10^{-4}, 1{\times}10^{-4}$, and $2{\times}10^{-5}$ M for $\Delta E_0 = -2, -4$, and $-6k_{\mathrm{B}}T$, respectively. This is within the typical binding site affinity range for proteins and sugar ligands.[5,6]

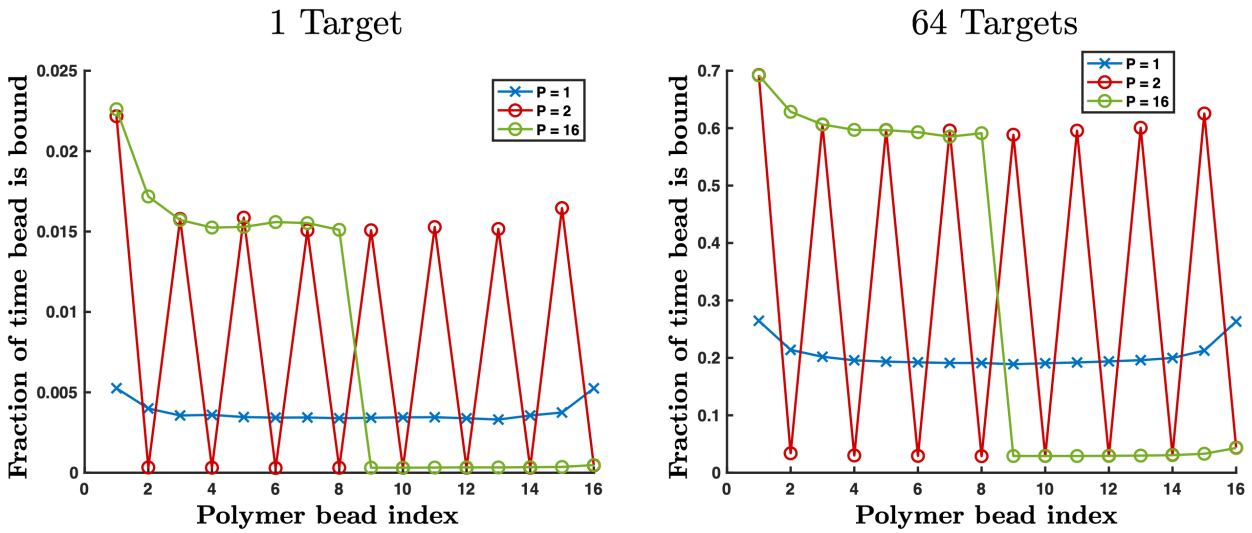

Figure S4: Frequency monovalent targets are bound to binding sites on homopolymers and copolymers with alternating and blocky patterns. Results are shown for (A) when a single target is placed with 4 16mer inhibiting polymers and (B) when 64 targets are placed with 4 16mer inhibiting polymers. Frequency of time bound depends on the affinity of that polymer binding site and not on polymer binding site pattern.

2 Monovalent binding frequency

In Figure S4, we have plotted the frequency each bead along the polymer chain is bound for monovalent targets to homopolymers $p = 1$, alternating heteropolymers $p = 2$, and blocky polymers $p = 16$. High affinity beads are bound with approximately the same frequency for all copolymer patterns. While the absolute fraction of time bound is different for low and high target concentrations, the qualitative results are the same. Monovalent targets bind to sites of the same affinity with the same frequency, regardless of copolymer pattern. The same is true of low affinity sites.

3 Other binding affinities

We also tested other binding affinities pairs both farther apart in energy $(0,-6k_{\mathrm{b}}T)$ and closer in energy $(-3,-5k_{\mathrm{b}}T)$. Without competition, dilute targets will still try to minimize the entropic cost of loop formation by binding to the two highest affinity sites, so we ex-

pect that in the dilute case blocky polymers will always be higher affinity than alternating polymers even with different binding affinity pairs. In competition with 64 targets, we also expect the same results as the main text for different binding affinity pairs, which we confirmed with simulation shown in Figure S5. In the case of competition, even when the low affinity sites go to $\Delta E_0 = 0 k_\mathrm{b} T$, we still see a lower K_D for the alternating polymer most likely due to the larger available free volume around the high affinity sites. Larger spacing between the high affinity sites gives unbound targets more free volume to approach and bind to the high affinity sites, even when they are already bound by competitors.

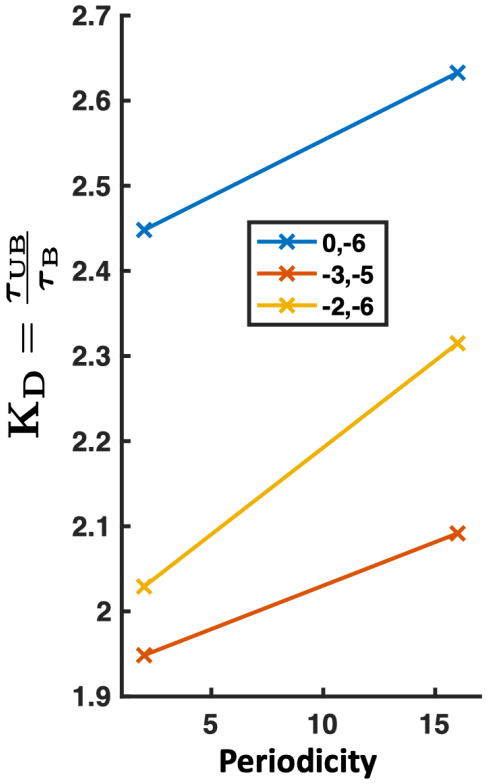

Figure S5: Dissociation constant for alternating ($p = 2$) and blocky ($p = 16$) polymers with ΔE_0 pairs (0,$-6 k_\mathrm{b} T$), (-2,$-6 k_\mathrm{b} T$), and (-3,$-5 k_\mathrm{b} T$). All data shown is for high competition simulations with 64 targets.

4 Effective target valency

We also thought it was interesting to examine how the target bonding changes as competition increases and with the polymer binding site pattern. In Figure S6, we have plotted

the fraction of all time bound that the target is bound divalently, as well as the fraction of time spent in each type of divalent bond. We show separately, the fraction of bound time the target spends with two high affinity ($-6k_{\mathrm{b}}T$) bonds, two low affinity bonds ($-2k_{\mathrm{b}}T$), and one of both low and high affinity bonds. From this plot we can see that as the blockiness or periodicity of the polymer increases, the total fraction of time spent bound divalently stays almost constant, but the types of divalent bonds change drastically. For example, in the 64 target case, two high affinity bonds account for 62% of all bonds for the blockiest copolymer, but only 41% of all bonds in the alternating polymer. Divalent bonds with both a high and low affinity bond follow the opposite trend. For the same 64 target concentration we can see that these combination bonds account for almost 28% of bonds in the alternating polymer and much less, only 7% of bonds in the blocky copolymer. These results align well with those presented in the main text showing that targets attempt to make divalent bonds with the polymer; the majority of all bonds formed are divalent. When bonding divalently, targets prefer to bind twice to high affinity beads, but also seek to decrease loop length. This can be seen by the lower number of two high affinity bonds for the alternating polymer than for the blocky polymer, and the increase in both low affinity/high affinity bonds for the alternating polymer over the blocky polymer.

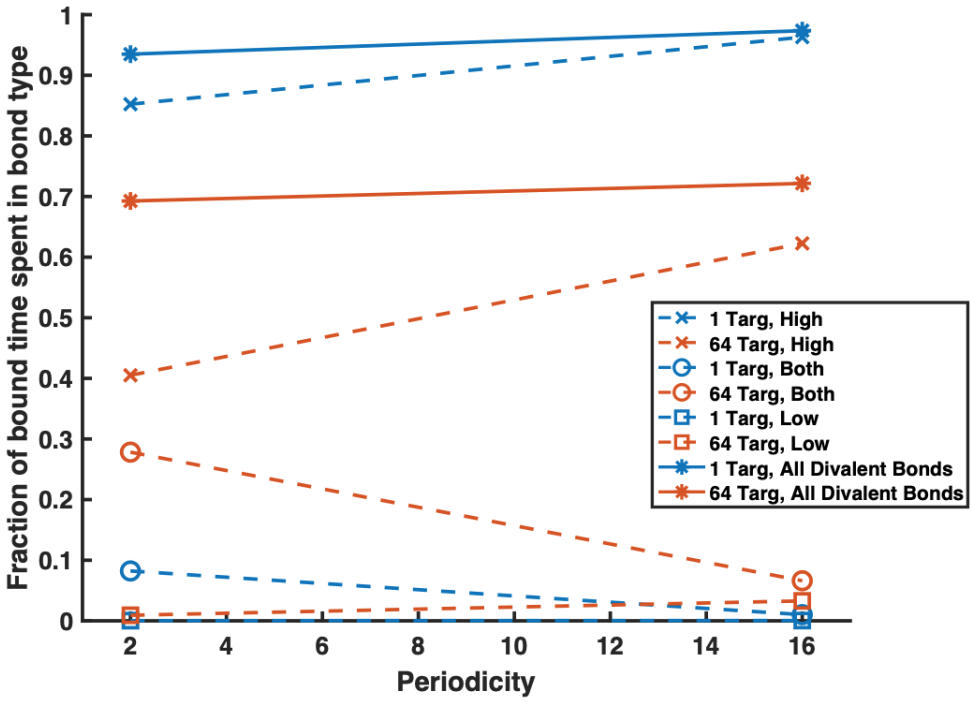

Figure S6: Fraction of all time spent bound that a target is bound divalently for a single target interacting with four polymers in orange (-∗) and for 64 targets interacting with polymers in blue (-∗). Fraction of time bound is also plotted for all three divalent bond types: two high affinity bonds (–x), two low affinity bonds (–□), and bonds with one low and one high affinity bonds, labeled as "Both" in the legend (–o). Values are shown for two polymer periodicities where ($p = 2$) is an alternating polymer and ($p = 16$) is a block copolymer.

References

(1) Berman, H. M.; Westbrook, J.; Feng, Z.; Gilliland, G.; Bhat, T. N.; Weissig, H.; Shindyalov, I. N.; Bourne, P. E. The Protein Data Bank. *Nucleic Acids Research* **2000**, *28*, 235–242.

(2) Ravishankar, R.; Thomas, C.; Suguna, K.; Surolia, A.; Vijayan, M. Crystal structures of the peanut lectin-lactose complex at acidic pH: retention of unusual quaternary structure, empty and carbohydrate bound combining sites, molecular mimicry and crystal packing directed by interactions at the combining site. *Proteins* **2001**, *43*, 260–270.

(3) Zumbro, E.; Witten, J.; Alexander-Katz, A. Computational Insights into Avidity of Polymeric Multivalent Binders. *Biophysical Journal* **2019**, *117*, 892–902.

(4) Targon Campana, P.; Ramos, L.; Barbosa, S.; Itri, R. Conformational stability of peanut agglutinin using small angle X-ray scattering. *International Journal of Biological Macromolecules* **2010**, *48*, 398–402.

(5) Chabre, Y. M.; Giguère, D.; Blanchard, B.; Rodrigue, J.; Rocheleau, S.; Neault, M.; Rauthu, S.; Papadopoulos, A.; Arnold, A. A.; Imberty, A.; Roy, R. Combining glycomimetic and multivalent strategies toward designing potent bacterial lectin inhibitors. *Chemistry - A European Journal* **2011**, *17*, 6545–6562.

(6) Lis, H.; Sharon, N. Lectins: Carbohydrate-Specific Proteins That Mediate Cellular Recognition. *Chemical Reviews* **1998**, *98*, 637–674.